An atomic model of the outer layer of the bluetongue virus core derived from X-ray crystallography and electron cryomicroscopy

Jonathan M Grimes[1†], Joanita Jakana[2], Mrinal Ghosh[3], Ajit K Basak[1‡], Polly Roy[3,4,5], Wah Chiu[2], David I Stuart[1,6*] and BV Venkataram Prasad[2*]

Background: Bluetongue virus (BTV), which belongs to the *Reoviridae* family and orbivirus genus, is a non-enveloped, icosahedral, double-stranded RNA virus. Several protein layers enclose its genome; upon cell entry the outer layer is stripped away leaving a core, the surface of which is composed of VP7. The structure of the trimeric VP7 molecule has previously been determined using X-ray crystallography. The articulated VP7 subunit consists of two domains, one which is largely α-helical and the other, smaller domain, is a β barrel with jelly-roll topology. The relative orientations of these two domains vary in different crystal forms. The structure of VP7 and the organization of 780 subunits of this molecule in the core of the virus is central to the assembly and function of BTV.

Results: A 23 Å resolution map of the core, determined using electron cryomicroscopy (cryoEM) data, reveals that the 260 trimers of VP7 are organized on a rather precise T = 13 *laevo* icosahedral lattice, in accordance with the theory of quasi-equivalence. The VP7 layer occupies a shell that is between 260 Å and 345 Å from the centre of the core. Below this radius (230–260 Å) lies the T = 1 layer of 120 molecules of VP3. By fitting the X-ray structure of an individual VP7 trimer onto the cryoEM BTV core structure, we have generated an atomic model of the VP7 layer of BTV. This demonstrates that one of the molecular structures seen in crystals of the isolated VP7 corresponds to the *in vivo* conformation of the molecule in the core.

Conclusions: The β-barrel domains of VP7 are external to the core and interact with the protein in the outer layer of the mature virion. The lower, α-helical domains of VP7 interact with VP3 molecules which form the inner layer of the BTV core. Adjacent VP7 trimer–trimer interactions in the T = 13 layer are mediated principally through well-defined regions in the broader lower domains, to form a structure that conforms well with that expected from the theory of quasi-equivalence with no significant conformational changes within the individual trimers. The VP3 layer determines the particle size and forms a rather smooth surface upon which the two-dimensional lattice of VP7 trimers is laid down.

Addresses: [1]The Laboratory of Molecular Biophysics, University of Oxford, Rex Richards Building, South Parks Road, Oxford OX1 3QU, UK, [2]Verna and Marrs McLean Department of Biochemistry and Keck Center for Computational Biology, Baylor College of Medicine, One Baylor Plaza, Houston, TX 77030, USA, [3]School of Public Health, University of Alabama at Birmingham, Birmingham, Alabama 35294, USA, [4]NERC Institute of Virology and Environmental Microbiology, Mansfield Road, Oxford OX1 3SR, UK, [5]Department of Biochemistry, University of Oxford, South Parks Road, Oxford OX1 3QT, UK and [6]Oxford Centre for Molecular Sciences, New Chemistry Building, South Parks Road, Oxford OX1 3QT, UK.

Present addresses: [†]EMBL Grenoble Outstation, c/o ILL, BP156, 38042 Grenoble, Cedex 9, France and [‡]Birkbeck College, Malet St, London WC1E 7HX, UK.

*Corresponding authors.
E-mail: dave@biop.ox.ac.uk
vprasad@bcm.tmc.edu

Key words: electron microscopy, orbiviruses, protein structure, virus structure

Received: 8 May 1997
Revisions requested: 22 May 1997
Revisions received: 5 June 1997
Accepted: 11 June 1997

Structure 15 July 1997, 5:885–893
http://biomednet.com/elecref/0969212600500885

Introduction

Members of the *Reoviridae* family are large, non-enveloped, segmented, double-stranded RNA (dsRNA) viruses with architecturally complex capsid structures. *Reoviridae* members include a number of human pathogens (e.g. the rotaviruses that cause diarrhoea), as well as other vertebrate, plant and insect viruses. Orbiviruses, which comprise a genus within the *Reoviridae* family, are vectored to vertebrate species (sheep, cattle and other animals) by arthropods (e.g. gnats, ticks, mosquitoes) and replicate in both types of host [1]. The ability of orbiviruses to infect a diverse range of hosts, and the complex molecular organization of the viral components, means that these viruses provide challenging systems to understand the structure–function relationships of complex viruses.

Bluetongue virus (BTV) is the best studied of the orbiviruses. It is approximately 800 Å in diameter and has multiple protein capsid layers enclosing its genome, which consists of 10 dsRNA segments, each coding for a single viral protein. Seven of these proteins are structural (being present in the mature virion), and of these VP2 and VP5 constitute a relatively loosely bound outer shell that is removed as the virus enters the host cell to produce an infection. The outer proteins may also be easily removed *in vitro* and the particle remaining is referred to in the literature as the core or single-shelled particle [2]. In the cytoplasm of the infected cell, the cores exhibit RNA-dependent RNA polymerase activity and indeed, given appropriate substrates, are capable of the sustained production of capped viral mRNA. The major protein constituents of the core are VP7 and VP3—VP7 forms an

outer capsid layer and VP3 a thinner inner layer. The genomic RNA and the other minor structural proteins, VP1, VP4 and VP6, are enclosed within the VP3 layer. Trimers of VP7 form the knobbly surface of the cores and are arranged on a T = 13 icosahedral lattice. The use of T numbers to describe the triangulation of an icosahedral surface, by the insertion of additional symmetry elements was described by Casper and Klug [3]. The number of subunits in such a lattice is 60T. Although the stoichiometry of VP7 (38 kD) in the virion (780 molecules per virion) has been conclusively derived from the structural studies [4], the stoichiometry of VP3 (103 kD) remained unclear for some time. Recently, biochemical studies indicated that there are 120 copies of VP3 per virion, corresponding to a VP7:VP3 stoichiometry of 13:2 [5].

Recently, we have performed several crystallographic analyses of BTV VP7 and also of a fragment of VP7 from another orbivirus, African horsesickness virus (AHSV); these are discussed in the accompanying paper, see Basak *et al.* in this issue of *Structure*. The VP7 subunit consists of two domains—a β-sandwich domain with the jelly-roll topology which is traditional amongst viral coat proteins [6] and the other domain is a bundle of α helices. The α-helical domain, consisting of nine helices, is almost twice as large (220 residues) as the β-sandwich domain (129 residues). The relative disposition of the two domains can differ wildly, depending on the crystal form. We have determined two structures for the intact VP7 trimer, in one structure the molecules measures some 85 Å along the molecular threefold axis by 65 Å in the other directions, whereas in the second crystal form the relative dimensions are inverted. In the accompanying paper (Basak *et al.* in this issue of *Structure*), we address the question of the stability and rigidity of the VP7 trimer, and suggest possible biological roles for such conformational flexibility.

The structure determinations of the individual VP7 molecule away from its natural T = 13 assembly in the virion raise several interesting questions. The first question to address is whether one, both or neither of the observed VP7 crystal structures are relevant to the structure of the core. We answer this question in this paper by fitting of the X-ray structures into a 23 Å resolution reconstruction of the core particle. The results show that one structure of the isolated molecule corresponds very closely to that seen at all quasi-equivalent positions on the core. This raises further questions. What is the precise orientation of the VP7 trimers in the virion? What are the interactions that stabilize the T = 13 icosahedral assembly? How does the VP7 molecule adopt to various quasi-equivalent environments in the T = 13 icosahedral lattice? How does VP7 interact with the outer capsid layer composed of VP2 and VP5, and with the inner capsid layer composed of VP3? We here provide answers to some of these questions. The theory underpinning these questions is that of quasi-equivalence [3], the central hypothesis of which is that chemically identical subunits can fit together in geometrically different positions on an icosahedrally symmetric surface by slight structural changes at the level of sidechain conformation. This has been shown to be invalid in many studies on a variety of plant and animal viruses [7,8,9]. From our results presented here, we find that the VP7 layer of BTV is emerging as an exceptional case where, at least at the level of detail of the current analysis, quasi-equivalence appears to be obeyed.

The Reoviridae have been the target for a number of crystallization studies and crystals suitable for X-ray analysis have been reported for rice dwarf virus [10], reovirus [11] and, most recently, for cores of BTV [5]. The analysis presented here, although not at atomic resolution, does provide an atomic model for a key component of a Reoviridae virion, which, in addition to the biological implications that can be deduced from it, will provide a firm framework for future analysis to higher resolution.

Results and discussion

The structure of the BTV core particle

The 3-dimensional (3-D) structure of the BTV-10 core particle was reconstructed from cryo-images of the virus particles embedded in a thin layer of vitreous ice. The specimen was imaged with a 400 kV electron microscope under low dose electron conditions, using a spot scan procedure (Figure 1). The 3-D structure of the BTV core particles

Figure 1

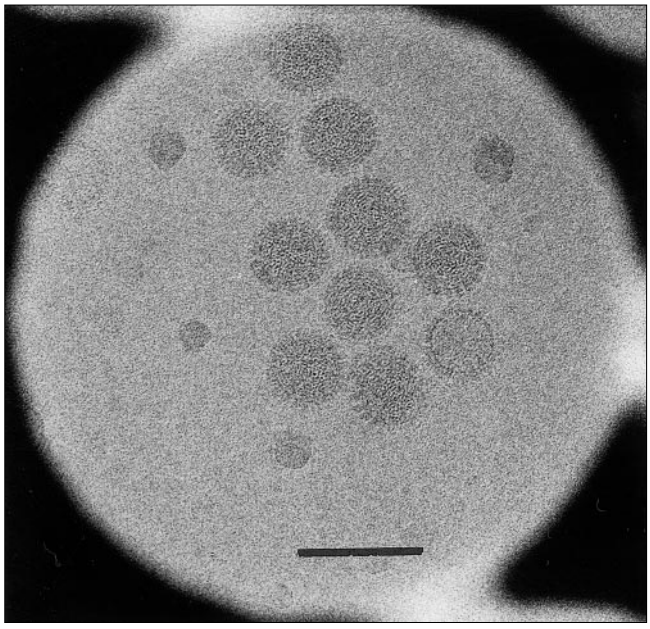

A typical portion of the cryoEM micrographs, imaged with a 400 kV electron cryomicroscope using a spot scan procedure, showing several cores (darker areas) embedded in a thin layer of vitreous ice. The scale bar shows 1000 Å.

Figure 2

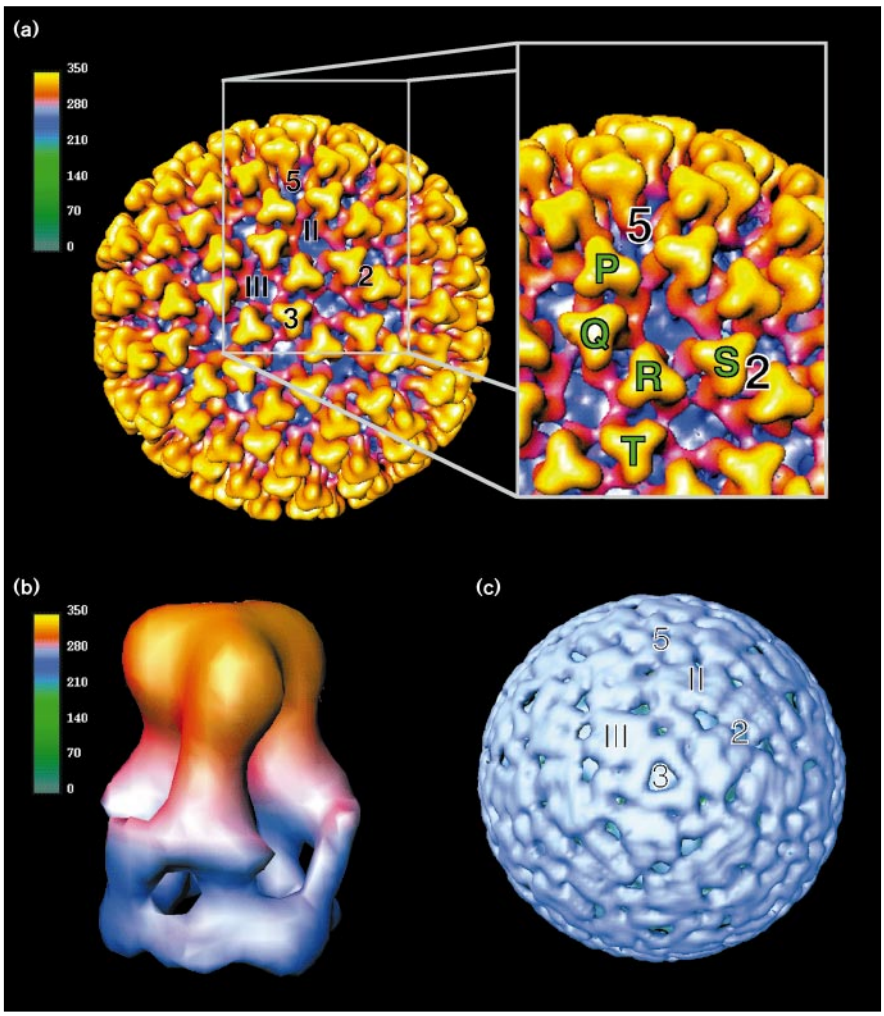

The overall cryoEM 3-D reconstruction of the core of BTV-10. (a) Surface representation of the core showing the trimers of VP7 in yellow, with an enlarged portion highlighting the protomeric unit of the viral capsid. The icosahedral axes are marked as are channels II and III in the layer of VP7. In the enlarged section, the five quasi-equivalent trimers are marked P (closest to the fivefold) to S (closest to the twofold axis) through to T (the trimer on the icosahedral threefold axis). (b) Close-up of a transverse view of a trimer of VP7 sitting on the inner layer of VP3, with the density coloured radially inward from yellow through to blue. (c) Figure of the cryoEM reconstruction of the core of BTV (radially cut at 260 Å), showing the smooth featureless inner layer of VP3 coloured in blue. The viral icosahedral axes and the positions of the channels II and III in the layer of VP7 are marked.

was computed, to a resolution of 23 Å, using Fourier-Bessel reconstruction, with 72 particles having unique orientations. At this resolution, 99% of the mean inverse eigenvalues of the 72 particles were less than 0.01, indicating that the data were adequately sampled in the Fourier space [12]. The extent to which the data obeyed icosahedral symmetry was evaluated by comparing the mean phase difference (phase residual) along cross common lines between Fourier transforms of particles, for all pairwise particle comparisons. The overall phase residual for our data was 54° (84° at 23 Å resolution). The effective resolution was estimated to be ~23 Å by computing the phase residuals and Fourier cross-correlation coefficients between two independent reconstructions, which were obtained by dividing the data set randomly into two sets. The phase residual between the two reconstructions reached 45° at a resolution of 23 Å. At this resolution, the Fourier correlation coefficient was –0.61. The surface representation of the 3-D map is shown in Figure 2a.

The T = 13 layer

As reported earlier, the outer layer of the core particle has a diameter of about 690 Å and exhibits T = 13 icosahedral symmetry [4]. In our current map, we clearly see a total of 260 triangular-shaped capsomers (VP7 trimers) that are arranged around large channels, which are found at all the five- and six-coordinated positions of the T = 13 lattice. These channels have been classified into three types based on their locations with respect to the icosahedral symmetry axes — type I channels run along the icosahedral fivefold axes, type II channels surround the fivefold axes, and the type III channels are located around the icosahedral threefold axes (Figure 2a).

The trimeric nature of the capsomers is better defined in the present higher resolution analysis than in previous studies of the BTV core; this has allowed the unique fitting of the high resolution X-ray structure of the trimer, as described in later discussions. It is necessary to define a

Figure 3

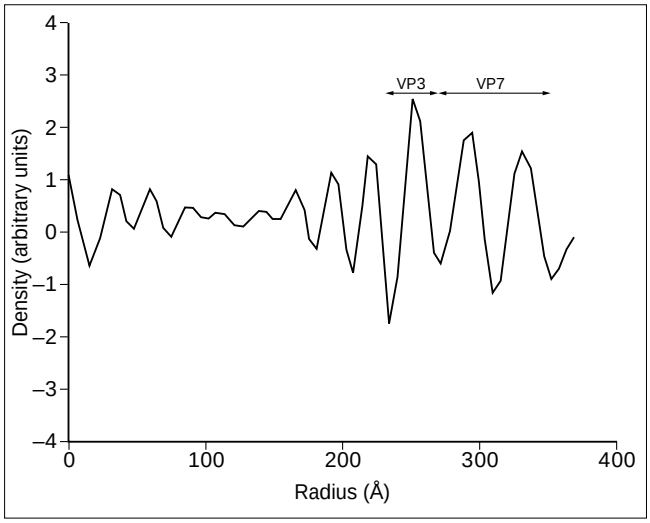

Radial density plot computed from the reconstruction of the BTV core. The radial extensions of the VP3 and VP7 layers are indicated.

more detailed nomenclature that will allow us to discuss the disposition of the individual polypeptide chains of VP7. Each asymmetric unit in the icosahedral lattice contains five quasi-equivalent trimers, designated P,Q,R,S and T as illustrated in Figure 2a. This nomenclature is designed to be as mnemonic as possible, thus, the peripentonal trimer (the one closest to the icosahedral fivefold axis) is labelled P and the others are labelled alphabetically according to their order proceeding outwards from the fivefold axis towards the trimer adjacent to the icosahedral twofold axis (trimer S) and finally the trimer located on the icosahedral threefold axis (T).

At the present resolution, no significant changes can be observed between the various quasi-equivalent trimers; this is reflected in the excellent fitting of the X-ray structure of VP7 to all trimers. The quality of the reconstruction can be judged from Figure 2b, which shows an icosahedral threefold capsomer excised from the 3-D map. At the distal end, the trimer has a triangular platform (yellow regions in Figure 2), which is formed by the closely interacting globular β-sandwich domains of the individual subunits. At a lower radius, ~300 Å, the mass density of the trimer clearly splits into three cylinder-shaped structures (coloured red in Figure 2), positioned at an angle to the threefold axis of the trimer. These structures correspond to the larger α-helical domain. Each cylinder-shaped structure curves laterally to interact with a subunit of the neighbouring trimer. The trimers are held together by a network of such interactions, as shown in Figure 2a. Each subunit extends further inward to interact with the inner capsid layer (blue in Figure 2) at a radius of 260 Å.

The T = 1 layer

The T = 13 icosahedral symmetry is clearly evident to an inner radius of 260 Å. Below this radius, the structure is presumed to have T = 1 icosahedral symmetry. This change in the structural organization signifies a change in the protein composition from VP7 to VP3. A surface representation of the structure at a radius of 260 Å is shown in Figure 2c. The channels seen in the T = 13 layer terminate at this radius. The surface morphology is relatively smooth with few indentations and small holes, which do not register with the broad channels in the T = 13 layer. Examination of the radial density profile indicates there is a distinct peak between ~230 Å and ~260 Å (Figure 3). The two peaks seen at ~290 Å and ~335 Å correspond to the two domains of the VP7 trimer. The volume occupied by the mass between the radii of 230 Å and 260 Å, assuming the contour level accounts correctly for 780 molecules of VP7 in the T = 13 layer, is consistent with 120 molecules of the 103 kD VP3. This is in agreement with the number proposed from biochemical studies [5]. It is not possible, however, to identify the positions of these two molecules of VP3, within the rather thin skin of density, which is inline with the much smaller mass of the VP3 layer (approximately 40% of the thicker and invaginated VP7 layer) requiring a more homogenous structure to ensure an adequate protection of the genome.

Fitting of the X-ray structure

Initially, we used the molecular graphics program FRODO [13] to fit the coordinates of a VP7 trimer into the electron-

Figure 4

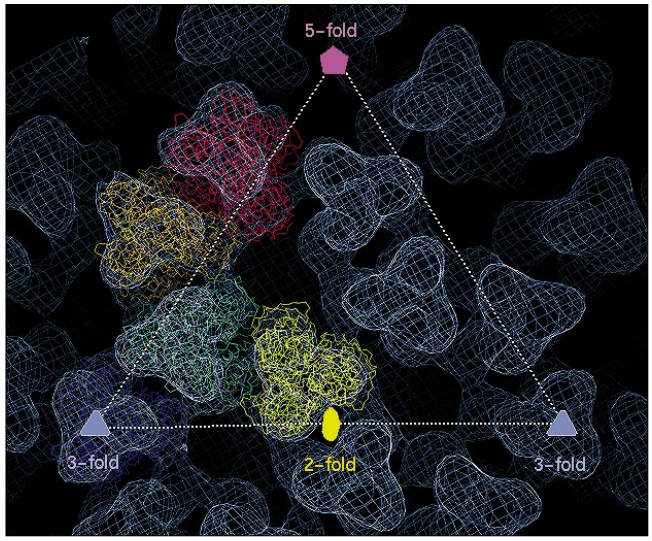

The optimized fit of five trimers of REF into the cryoEM density reconstruction of the core of BTV-10. The Cα trace is shown for each trimer, coloured as follows: P, red; Q, orange; R, emerald; S, yellow; and T, blue. (Figure produced using FRODO [13].)

density distribution of the reconstruction by simple visual inspection. At this stage, a structure was known for the intact VP7 trimer of BTV (both the reconstruction and the crystal structure of the type 10 virus)—that described by Grimes *et al.* [14] and denoted REF (for reference structure) in the accompanying paper (Basak *et al.* in this issue of *Structure*). By visual observation of the cryoEM map, we positioned a copy of this trimer in each of the five independent positions within the icosahedral asymmetric unit. All fits appeared reasonable and, in order to optimize them objectively, we refined the orientations by real-space refinement. The method, which used a simple steepest-ascent algorithm to maximize the correlation coefficient between the observed cryoEM density and electron density calculated from the atomic model, was implemented in the program GAP (JMG & DIS, unpublished data) and is described in the Materials and methods section. The procedure worked well—the shifts were sensible when checked visually and deliberate misalignment followed by re-refinement showed that the maxima detected by the refinement method were, at least locally, unique. The refined fits for all of the trimers were excellent, as judged both visually and in terms of the real space correlation coefficients (which varied from 89% to 90%). Figure 4 shows the overall fit (after optimization) of trimers PDT, and Figure 5a shows the optimized fit of trimer T to the cryoEM density. The initial visual fitting convinced us that the relative up/down orientation of the VP7 molecule, with respect to the centre of the particle, was correct and that the orientation of the trimers around the local threefold axes was uniquely defined. We confirmed this by performing density correlation tests, as described in the Materials and methods section. There remained a further, potentially serious, ambiguity, namely in the tertiary and quaternary states of the molecules. A second, radically different, conformation for the VP7 trimer has been

Figure 5

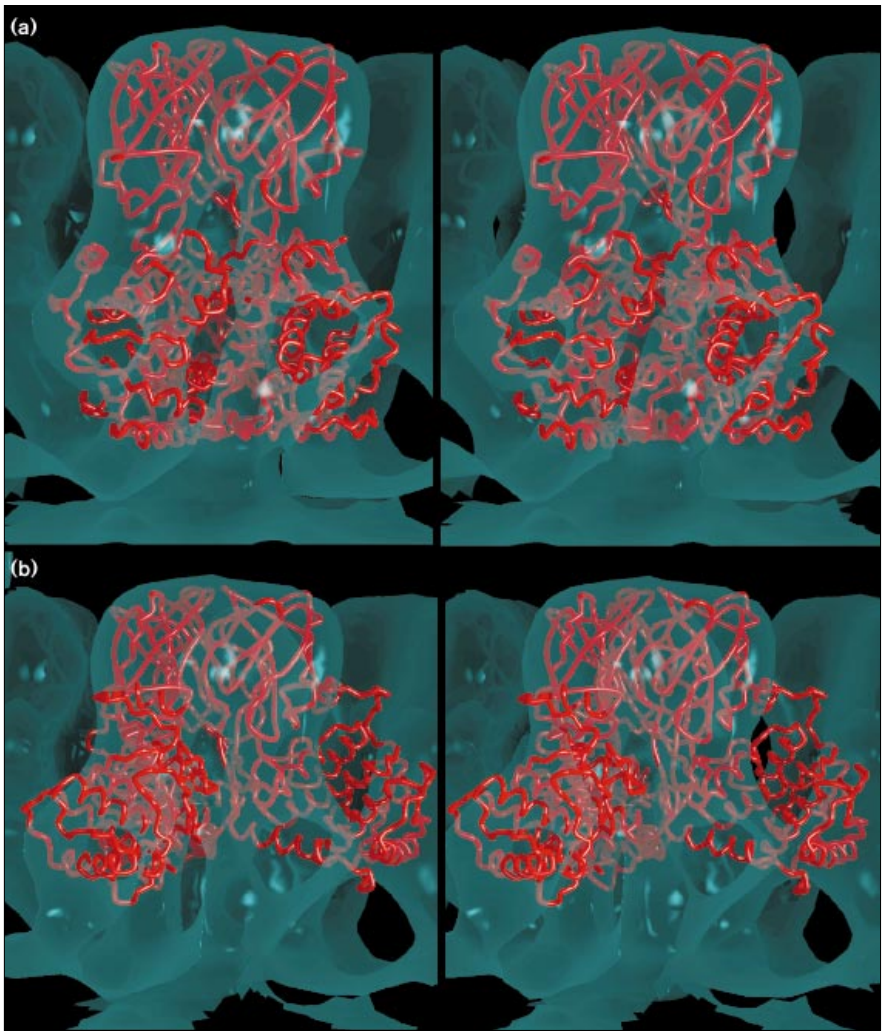

Stereo images of the structures of the two trimers of VP7 (REF and HEX, see accompanying paper Basak *et al.* in this issue of *Structure*) fitted to the cryoEM reconstruction of the BTV core, solved to a nominal resolution of 23 Å. (a) The optimum fit of the structure of REF, represented as a red coil, to the cryoEM density for the trimer of VP7 (coloured as a slate-blue semi-transparent surface) on the icosahedral threefold axis of the viral core. This fit gave a linear correlation coefficient of 90% between the calculated electron density and the cryoEM density. (b) The fit of HEX, coloured as a red coil, to the cryoEM density for the trimer of VP7 sitting on the viral icosahedral lattice (coloured slate-blue), showing the markedly worse fit of HEX than REF to the cryoEM reconstruction. (Figure produced using the programs BOBSCRIPT (R Esnouf, personal communication), extensively modified from MOLSCRIPT [27] and rendered with RASTER3D [28,29].)

Figure 6

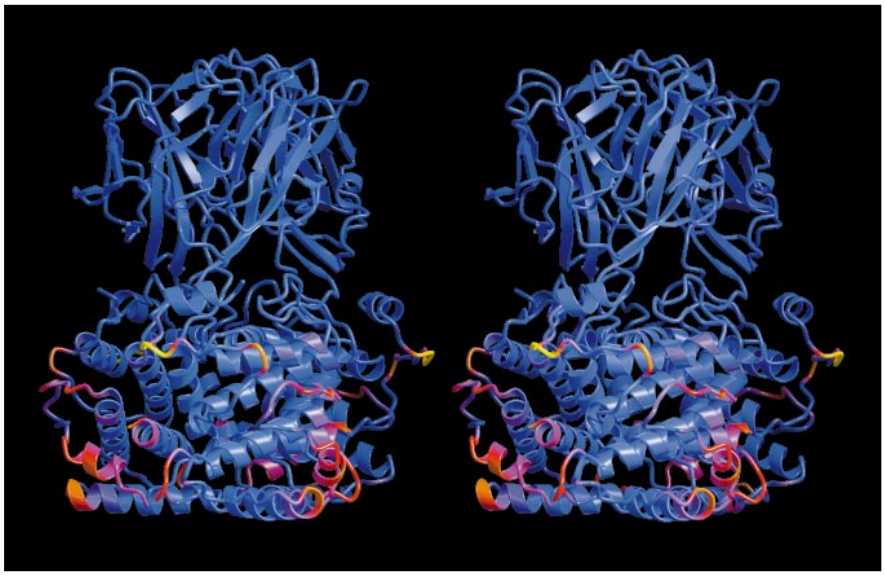

Fold of the trimer of VP7 colour-coded to highlight the areas of VP7 involved in trimer–trimer interactions. There are 13 different sets of interactions between the trimers on the core surface, P–Q, Q–P, Q–R, R–Q, R–S, S–R, R–T, T–R plus P–P′, P′–P, S–Q′, Q′–S and S–S′, where the primes refer to icosahedral symmetry-related trimers. Each trimer was examined in turn and those residues in any one subunit of the trimer within 8 Å of a residue in a contacting dimer were marked as being in the contact region. The sum was taken, over all the trimers, of the number of occasions each residue was contacted. This was then mapped onto the fold of the trimer, coloured from blue (0–1 contacts) through to yellow (greater than 11 contacts). (Figure produced using the programs BOBSCRIPT and RASTER3D [28,29].)

determined (denoted HEX) and its structure is described in the accompanying paper, see Basak *et al.* of this issue of *Structure*. The top domains remain unchanged between REF and HEX, whereas the lower domains move outwards and rotate about the linker regions between the two domains by some 160°. A further test, also described in the Materials and methods section, was performed to establish if we could distinguish the trimer structure actually present in the core. The result was conclusive—all trimers on the core surface are in the REF type conformation. The β domain of the VP7 structure corresponds to the distal globular portion of the trimer density in the cryo-EM map with the α-helical domains sitting below and interacting with the VP3 layer.

VP7 trimers in the core are indistinguishable from those in the crystal

The quality of the fit of the atomic coordinates to the reconstruction (which may be judged from Figures 4 and 5) allows us to state that, to the precision of the reconstruction, the structures of all 260 VP7 trimers which form the outer layer of the viral core are in the REF conformation. Thus, at the level of detail of this analysis, VP7 does not undergo any significant conformational changes upon adopting these quasi-equivalent locations on the T = 13 lattice.

Fitting the X-ray structure of individual trimers to the EM reconstruction has given us a crude atomic model for the VP7 layer of the core. What accuracy can we expect such a model to possess? Combining a large amount of precise information together during the rigid body refinement should confer an accuracy on the model that is far higher than the resolution of the reconstruction. By analogy with the resolution:accuracy ratio obtained for high resolution X-ray analyses (where chemical restraints are analogues of the rigid body constraints), we expect the model to have a mean error of perhaps 4 Å. This is not sufficient to allow the chemical details of molecular interactions to be mapped at the atomic level, nevertheless, we should be able to delineate, at the level of amino acids rather than individual atoms, the regions in the VP7 polypeptide that are involved in the inter-trimeric interactions. In addition, we should be able to comment on some aspects of the interaction between the VP7 and VP3 molecules. In the absence of a reconstruction of the intact virus at a resolution comparable to that of the core, we will not speculate about the interactions between the VP7 and outer layers beyond the discussion in Grimes *et al.* [14].

A T = 13 lattice of some perfection

The distances between the centres of gravity of the five unique trimers and the centre of the particle vary between 289 Å and 299 Å, with the trimers on the icosahedral threefold axes (T trimers) being closest to the particle centre and the P trimers being the furthest from the centre, which is as expected for a structure possessing some icosahedral character. We have noted that there is little evidence of any conformational flexibility within the VP7 trimers *in situ* on the core. This is reflected in the regularity of the disposition of the trimers on the surface of the core. These adjacent trimers are related by rotation axes that are almost perpendicular to the VP3 layer and deviate by no more than 10° from exact twofold symmetry. These pseudo-twofold interactions define the contacts between trimers. This is analysed in Figure 6 and it is notable that the interactions tend to be rather

hydrophobic and are disposed in relatively compact patches on the trimer surfaces. The main area of interaction between trimers of VP7 is located on one side of the monomer and is primarily made up of the extended loop 76–79 (GINVGP), helix 4 (secondary structure definition given in Grimes *et al.* [14]) which comprises residues 88–97 (MATIGVLATP) and the end of helix 2 (residues 42–44, GLT). A short loop 20–22 (EAR) at the end of helix 1 and loop 334–339 (PMPGP), preceding the C-terminal helix, from a threefold related subunit within the trimer also make a smaller but significant contribution. This commonality of interaction across the protomeric unit of BTV suggests how the seeming complexity of a T = 13 lattice can be achieved. Trimers of VP7 have a natural propensity to form hexagonal lattices, thus, Burroughs *et al.* [15] observed microcrystals of VP7 in the cytoplasm of cells infected with African horsesickness virus (whose VP7 is structurally very similar to that of BTV, [16]). We propose that this hexagonal lattice, made up of trimers of VP7 forming pseudo-twofold dimers, is the starting point for defining the T = 13 lattice, because in the electron micrographs, the dimensions of the hexagonal rings in the microcrystals and on the core surface appear to be indistinguishable (P Mertens, personal communication). By inserting fivefold axes at appropriate points in the hexagonal lattice, the T = 13 lattice is generated, but the driving force or mechanism for this change of symmetry from pseudo-sixfold to fivefold is unclear. It nevertheless seems highly implausible that switching of symmetry occurs due to self-driven conformational switching in VP7. This implies that VP3, which is known to self-assemble to form single-shelled particles [17], defines the size of the virus and thus supplies the information necessary to force closure of the flat hexagonal lattice of VP7 onto the icosahedral lattice of the particle. The atomic B factors of the REF crystal structure suggest that the C-terminal regions of VP7 are relatively flexible, however, at the resolution of the present study, we cannot judge whether these regions act as mobile arms capable of modulating the interactions between adjacent trimers and we see no evidence for this occurring.

As the nature of the underlying layer of VP3 is still unclear, we cannot speculate on how 780 copies of VP7 interact with 120 copies of VP3. We can, however, say something about the nature of the surface of VP7 that interacts with VP3. We have already noted [14] that the surface is predominantly hydrophobic in character and extremely flat, thus, presumably facilitating the symmetry mismatch in packing that needs to occur on viral assembly, possibly, by allowing some degree of flexing in terms of the specificity of interactions between the molecular surfaces. We are now able to say that any such flexing must be subtle, because it cannot be detected at this resolution and it is likely to be largely achieved by sidechain rearrangements.

Biological implications

Bluetongue virus (BTV) belongs to the *Reoviridae* family of double-stranded RNA viruses. Among this family of viruses are several human and animal pathogens including rotavirus, a major pathogen of infantile gastroenteritis. A structural feature, common to members of this family of viruses, is a multilayered capsid formed by several concentric layers of different protein compositions. The intricate nature of the molecular interactions that leads to such a complex assembly is far from understood. The outer shell proteins are removed as the virus enters the host cell, leaving the viral core. The major protein constituenents of the core are VP7 and VP3: VP7 forms an outer layer and VP3 a thinner inner layer. In the present study, we have used a combination of X-ray crystallography and electron cryomicroscopy (cryoEM) to provide a better understanding of the molecular interactions in a T = 13 layer, which is formed by 260 trimers of VP7 in the BTV core, and the interactions of this layer with the underlying T = 1 layer formed by VP3 molecules.

Pooling information from cryoEM and X-ray crystallography is extremely powerful, as it allows the accurate positioning (to within 4 Å) of macromolecules in a relatively large complex and the precise mapping of chemical information onto otherwise chemically obscure electron-density reconstructions. In this way, we have obtained an initial model for the outer layer of the BTV core, enabling us to suggest possible sites of interaction between the trimers of VP7 that make up this rather complex structure.

The model throws light on the relevance of the theory of quasi-equivalence for the assembly of very complex systems [3]. This theory rests on the hypothesis that chemically identical molecules fit together in almost equivalent ways to make a viral capsid of structural integrity simply by minor structural changes, at the level of sidechain conformation, in the intermolecular interfaces. There are two major problems with the theory. Firstly, it does not provide an explanation of how the size of the virus is defined. This problem may be solved by conformational switching, which allows the system to be self-measuring. The most complex example of this, to date, is the pseudo T = 7 assembly seen in SV40 [9]. An alternative mechanism, not yet observed in atomic detail, is the use of a scaffold of other proteins to size the assembly [18]. The second problem is one of distortion. This arises because a substantial surface of subunit–subunit interaction is needed to achieve a robust capsid, implying that these interactions span a significant radial depth. The relative tilting of subunits in going from five to sixfold axes will then strain the interaction beyond what can be accommodated by sidechain rearrangements. These problems have led to the expectation that the theory of quasi-equivalence is inapplicable at the atomic level. The great

complexity of the BTV core means that very intricate conformational switching would be needed to control the VP7 assembly. Instead, we believe that VP3, which can self-assemble to form a subcore, fulfills the measuring role by acting as a permanent scaffold. VP3, which is only present in 120 copies, cannot obey the rules of quasi-equivalence as T=2 triangulation is not allowed; further analysis is required to resolve VP3's part in the puzzle. The distortion problem appears to be overcome, or ameliorated, by partitioning the VP7 interactions into two distinct sets. A two-dimensional interaction with flat regions on the VP3 substrate locks VP7 onto the subcore, whereas discrete regions of VP7 interact to lock the trimers together in a pairwise fashion, thus, providing the relative articulation needed to accommodate the T = 13 lattice distortions which lead to the observed variation in radial disposition of the trimers. A higher resolution structure is required to establish the extent to which residual conformational switching of the VP7 trimers occurs in the different quasi-equivalent environments.

Materials and methods

Virus and cells

United States prototype BTV type 10 (CA-10) was plaque cloned, using monolayers of BHK-21 cells. The mature virus and the core particles were obtained essentially as described previously by Prasad *et al.* [4].

Electron cryomicroscopy

Specimen preparation for electron cryomicroscopy was carried out using the technique described by Dubochet *et al.* [19]. A small amount of sample (~4 μl) was applied to one side of a holey carbon grid. Excess liquid was blotted away from the grid with filter paper and the grid was immediately plunged into a bath of liquid ethane, which was maintained at –179°C by surrounding liquid nitrogen. The frozen-hydrated specimen grid was transferred under liquid nitrogen to a GATAN cryostation and placed into a GATAN cryoholder for imaging. The specimen was imaged in a 400 kV electron microscope (JEOL 4000) at a magnification of 30 000X using spot scan procedures [20,21,22] with low electron dose (~5 $e^-/Å^2$ on the specimen). Images were recorded in focal pairs, at applied values of ~2.5 and ~3.0 mm underfocus. Micrograph pairs were chosen for image analysis on the basis of the defocus, the number and distribution of virus particles and the ice thickness. Selected electron micrograph pairs were digitized using a Perkin Elmer microdensitometer with a step size that corresponded to 5.33 Å/pixel in the object, and transferred to a Silicon Graphics workstation for subsequent image processing.

3-D reconstruction procedures

Particles from both images of the digitized focal pair were boxed into individual particle images with a pixel area of 256×256. Each particle image then was floated and masked with a suitable radius. The closer-to-focus particles were used to compute the 3-D reconstruction, whereas the further-from-focus particles confirmed the orientations of the corresponding closer-to-focus particles. Orientation determination of the particles using self-common lines [12] and subsequent orientation refinement using cross-common lines [23] were carried out as described previously [24]. The final reconstruction was computed using the cylindrical expansion method [12] to a resolution of 23 Å, which contained information within the first zero of the contrast transfer function. No correction was made for the effects of contrast transfer function. The actual defocus value of the closer-to-focus micrograph was estimated to be 2.6 μm from the sum of the Fourier transforms of the individual particles [21]. To determine the effective resolution, Fourier cross correlation coefficients and phase residuals were computed, using equations 3 and 6, respectively, in van Heel [25], between reconstructions obtained by randomly dividing the data into two sets. Explorer Graphics software (NAG Inc.) with additional customized modules (Lawton JA and BVVP, unpublished data) was used to visualize and manipulate the 3-D map.

Real-space fitting

Initial fitting of X-ray structures to the cryoEM reconstruction was performed by manual manipulation using FRODO [13] and an Evans and Sutherland ESV graphics workstation. The initial fits were obtained using the REF crystal structure of the VP7 trimer [14] (see also accompanying paper Basak *et al.* in this issue of *Structure* for definition of nomenclature for different VP7 structures). Further fitting was achieved by matching the calculated electron density distribution at a resolution of 24 Å for the trimer of VP7 to the electron density from the reconstruction for the five unique trimers on the core surface that define the icosahedral protomeric unit ($4^1/_3$ trimers define the T = 13, protomeric unit of the particle, but it is convenient to analyse five trimers, including the trimer on the icosahedral threefold axis). The algorithm used (implemented in program GAP; JMG and DIS, unpublished data) was a steepest ascent refinement procedure which optimizes the linear correlation coefficient between the two electron densities. To avoid a distortion of the calculated electron density for the model of VP7 *in vacuo* at 24 Å, due to series termination ripple effects, a solvent correction was applied in XPLOR version 3.1 [26], followed by application of an appropriate B factor to the structure factors prior to map calculation. A series of tests were carried out in XPLOR to see what combination of solvent correction and B factor produced the optimum agreement with the cryoEM density. Several maps were calculated with the solvent mask set to values between 0 and 0.33 $e^-/Å^3$, with overall B factors varied from 100 to 3000 $Å^2$ for each map. By this procedure, it was found that setting the solvent level to 0 $e^-/Å^3$ and applying an overall B factor of 500 $Å^2$ gave the best starting correlation coefficient. Although we note that these quantities should not be interpreted in any physical sense, they will reflect various effects, such as radiation damage, inexact orientations for the particles and incomplete contrast transfer function correction. This map was used subsequently in all calculations. Approximate matrices to superimpose the cryoEM densities of the five unique trimers of VP7 onto the calculated density distribution were derived from the relationships of the Cα atoms of the trimer used to calculate the electron density at 24 Å and coordinates of the trimers roughly positioned into the cryoEM reconstruction. At this resolution a 3-D reconstruction of a protein has little internal structure and is best described as a shape function (DIS and JMG, unpublished data). To ensure that maximal definition of this shape was included in the optimization of the correlation coefficient, a mask was used to filter the pixels, derived from the coordinates of VP7, with every pixel within 10 Å of an atom being included. Thus, a layer of solvent was included in the refinement, the shape function being defined by the protein/solvent boundary.

The fitting procedure resulted in very good final correlation coefficients of between 89% and 90% for the five trimers (increases from start values of between 87% to 88%). Four tests were performed to check the uniqueness of these results. The first test involved calculating the correlation coefficients between the cryoEM density for one of the trimers (the trimer on the icosahedral threefold axis, but it could have been any of the others) and the calculated density, rotated in increments of 10° around the molecular threefold axis away from the optimized fit. The results of this test are presented in Figure 7 and show a clear single optimum corresponding to the position found by the above refinement procedure. The second test was to calculate the correlation coefficient between the cryoEM density and the calculated density but for the test trimer rotated by 180° about an axis tangential to the surface of the core, from its optimized fit (i.e. so the α-helical domains in the model now resided in the density corresponding to the β-sheet domain). This resulted in a reduction in the correlation coefficient to 78%, which on refinement increased to 85%. These tests indicate that one can easily distinguish the optimized orientation of the model from alternative fits and suggests that the fitting procedure is likely to have found a global optimum. The third test was designed to investigate

Figure 7

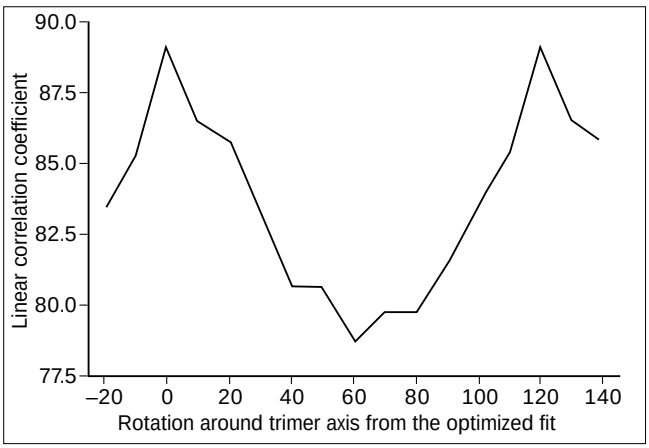

Graph showing the variation of linear correlation coefficient between the cryoEM data and X-ray data of VP7, as one applies successive 10° rotations around the molecular threefold axis of the oligomer.

whether we could distinguish between the REF and HEX trimer structures. These structures are radically different in the relative disposition of the two domains of the VP7 subunits. The HEX structure was orientated so the invariant trimeric jelly-roll domains superimposed with the domains of the optimally fitted REF structure. This fit gave a correlation coefficient of 67.4%, again confirming that our procedure is capable of some discrimination between the two crystal forms. The approximately equal correlation coefficients for the five trimers means that we can be confident that each of them is in the REF conformation and in the orientation and position produced by the refinement procedure. To make sure that no intermediate structure between REF and HEX is found *in situ* on the core surface, the fourth test involved refining the top domain alone against the cryo-EM density. This fitting gave an identical position to that obtained with the whole of VP7 (structure REF), indicating that there was no evidence for an intermediate conformation.

Accession numbers

The atomic coordinates for the model of the core will be deposited at the Brookhaven Protein Data Bank and are available from the authors.

Acknowledgements

We are grateful to Peter Mertens for helpful discussions. Stephen Lee for advice and practical help with digital imaging, to Robert Esnouf and Richard Bryan for help with computing and to Jeff Lawton for help with EXPLORER modules. This project was supported by the NIH (grants A136040 to BVVP and RR2250 to WC) and by the BBSRC. The Oxford Centre for Molecular Sciences is supported by the BBSRC, MRC and EPSRC. DIS is supported by the MRC.

References

1. Knudson, D.L. & Monath, T.P. (1990). Orbiviruses. In *Virology.* (Fields, B.N., Ed), pp. 1405–1436, Raven Press, New York.
2. Fields, B.N. (1996). Reoviridae. In *Virology.* (Fields, B.N., Knipe, D.M. & Howley, P.M., Eds), pp. 1553–1555, Lippincott-Raven, Philidelphia.
3. Casper, D.L.D. & Klug, A. (1962). Physical principles in the construction of regular viruses. *Cold Spring Harbor Sym. Quant. Biol.* 27, 1–22.
4. Prasad, B.V., Yamaguchi, S. & Roy, P. (1992). Three-dimensional structure of single-shelled bluetongue virus. *J. Virol.* 66, 2135–2142.
5. Burroughs, J.N., Grimes, J.M., Mertens, P.P. & Stuart, D.I. (1995). Crystallization and preliminary X-ray analysis of the core particle of bluetongue virus. *Virology* 210, 217–220.
6. Stuart, D.I. (1993). Viruses. *Curr. Opin. Struct. Biol.* 3, 167–174.
7. Harrison, S.C., Olson, A., Schutt, C.E., Winkler, F.K. & Bricogne, G. (1978). Tomato bushy stunt virus at 2.9 Å resolution. *Nature* 276, 368–373.
8. Hogle, J.M., Chow, M. & Filman, D.J. (1985). Three-dimensional structure of poliovirus at 2.9 Å resolution. *Science* 229, 1358–1365.
9. Liddington, R.C., Yan, Y., Moulai, J., Sahli, R., Benjamin, T.L. & Harrison, S.C. (1991). Structure of simian virus 40 at 3.8 Å resolution. *Nature* 354, 278–284.
10. Mizuno, H., Kano, H., Omura, T., Koizumi, M., Kondoh, M. & Tsukihara, T. (1991). Crystallization and preliminary X-ray study of a double-shelled spherical virus, rice dwarf virus. *J. Mol. Biol.* 219, 665–669.
11. Coombs, K.M., Fields, B.N. & Harrison, S.C. (1990). Crystallization of the reovirus type 3 Dearing core. Crystal packing is determined by the lambda 2 protein. *J. Mol. Biol.* 215, 1–5.
12. Crowther, R.A., DeRosier, D.J. & Klug, A. (1970). The reconstruction of a three-dimensional structure from projections and its application to electron microscopy. *Proc. R. Soc. Lond A* 317, 319–340.
13. Jones, T.A. (1985). Interactive computer graphics: FRODO. Diffraction methods for biological macromolecules. In *Methods in Enzymology.* (Wyckoff, HW., Hirs, CHW. & Timasheff, SN., eds), pp. 157–171, Academic press, Orlando.
14. Grimes, J.M., Basak, A.K., Roy, P. & Stuart, D.I. (1995). The crystal structure of bluetongue virus VP7. *Nature* 373, 167–170.
15. Burroughs, J.N., *et al*., & Mertens, P.P.C. (1994). Purification and properties of virus particles, infectious subviral particles, cores and VP7 crystals of African horsesickness virus serotype 9. *J. Gen. Virol.* 75, 1849–1857.
16. Basak, A.K., Gouet, P., Grimes, J.M., Roy, P. & Stuart, D.I. (1996). Crystal structure of the top domain of African horsesickness VP7. Comparisons with Bluetongue virus VP7. *J. Virol.* 70, 3797–3806.
17. Huismans, H., van Dijk, A.A. & Els, H.J. (1987). Uncoating of parental bluetongue virus to core and subcore particles in infected L cells. *Virology* 157, 180–188.
18. Ilag, L.L., *et al.*, & Incardarno, N.L. (1995). DNA packaging intermediates of bacteriophage PhiX174. *Structure* 3, 353–363.
19. Dubochet, J., Adrian, M., Chang, J.J., Homo, J.C., Lepault, J. & McDowall, A.W. (1988). Cryo-electron microscopy of vitrified specimens. *Quart. Rev. Biophys.* 21, 129–228.
20. Brink, J., Chiu, W. & Dougherty, M. (1992). Computer controlled spot scan imaging of crotoxin complex crystals with 400 keV electrons at near atomic resolution. *Ultramicroscopy* 46, 229–240.
21. Zhou, Z.H., Prasad, B.V.V., Jakana, J., Rixon, F.J. & Chiu, W. (1994). Protein subunit structures in the herpes simplex virus A-capsid determined from 400 keV spot scan electron cryomicroscopy. *J. Mol. Biol.* 242, 456–469.
22. Prasad, B.V.V., *et al.*, & Estes, M. K. (1996). Visualisation of ordered genomic RNA and localisation of transcriptional complexes in rotavirus. *Nature* 382, 471–473.
23. Fuller, S.D. (1987). The T = 4 envelope of Sindbis virus is organised by interactions with a complimentary T=3 capsid. *Cell* 48, 923–934.
24. Lawton, J.A. & Prasad, B.V.V. (1996). Automated software package for icosahedral virus reconstruction. *J. Struct. Biol.* 116, 209–215.
25. van Heel, M. (1987). Similarity measures between images. *Ultramicroscopy* 21, 95–100.
26. Brunger, A.T. (1992). *X-PLOR Version 3.1*. Yale University Press.
27. Kraulis, P.J. (1991). MOLSCRIPT: a program to produce both detailed and schematic plots of protein structure. *J. Appl. Cryst.* 24, 946–950.
28. Merrit, E.A. & Murphy, M.E.P. (1994). Raster3D version 2.0. A program for photorealistic molecular graphics. *Acta Cryst.* D 50, 869–873.
29. Bacon, D.J. and Anderson, W.F. (1988). A fast algorithm for for rendering space-filling molecule pictures. *J. Mol. Graphics* 6, 219–220.